Energy loss of a charged particle in a magnetized quantum plasma

M. Steinberg and J. Ortner
Institut für Physik, Humboldt Universität zu Berlin, Invalidenstraße 110, D-10115 Berlin, Germany
(Received 5 June 2000; published 21 March 2001)

This paper investigates the stopping power of a weakly coupled magnetized plasma. The effect of the Larmor rotation of the heavy charged test particle is carefully analyzed. The dielectric formalism is employed to obtain a general expression for the stopping power. A quantum mechanical form of the random-phase approximation dielectric function is used so that an abitrary cutoff procedure is not required. Simple analytical expressions for the stopping power have been found for the cases of high and low projectile velocity of the test particle. The dependence of the stopping power on the angle of incidence is studied. A comparison with numerical solutions is given. It is found that in general a magnetic field reduces the stopping power of the plasma at high velocities, while it increases the stopping power at low velocities.

DOI: 10.1103/PhysRevE.63.046401 PACS number(s): 52.40.Mj, 52.35.Hr, 52.25.Fi, 05.20.Dd

I. INTRODUCTION

There have been a number of theoretical studies of the ion beam stopping power of a plasma. Although some calculations of the stopping power in a magnetized plasma have been presented in the early 1960s [1,2] the topic has only recently become of general interest [3–5]. Partly, this is due to the fact that strong magnetic fields are now experimentally available [6]. The experimental motivation for this investigation also comes from the heavy-ion fusion research, in which the experiments are usually carried out in the presence of a magnetic field. We also mention the importance of this topic in connection with the efforts to model the atmosphere of magnetized white dwarfs and magnetized neutron stars, on the surface of which the magnetic field can be as high as 10^5-10^{14} kG.

Some progress has been recently made in the calculation of the thermodynamic properties of quantized magnetized plasmas. The low-density magnetized plasma system has been tackled in the works of Cornu [7], Boose and Perez [8], and of Steinberg *et al.* [9]. The ground state energy of a degenerate strongly magnetized plasma has been investigated by Skudlarski and Vignale [10] and by Steinberg and Ortner [11]. The plasma diagnostics on the basis of scheduled experiments investigating the interaction of a laser or a particle beam with a magnetized plasma require the knowledge of the dielectric function. The dielectric tensor of a magnetized coupled plasma has been studied in recent works [12–14].

In this paper we study the stopping power of a charged projectile passing a magnetized plasma. In order to simplify the calculations we focus on the case of a weakly coupled magnetized plasma. A weakly coupled plasma is characterized by a small coupling parameter Γ, which is given by

$$\Gamma = \frac{e^2}{4\pi\epsilon_0 kTd}, \tag{1}$$

where $d=(3/4\pi n)^{1/3}$ is the mean distance between the particles and T is the temperature of the plasma. Since the pioneering work of Lindhard [15], the theory of the stopping power of a (weakly or strongly coupled) plasma was considered within the framework of the dielectric formalism. It was found that the stopping power, i.e., the energy loss per unit length of the projectile, and the dielectric function of the plasma $\epsilon(\mathbf{q},\omega)$ are related by the formula

$$S = \frac{1}{u}\left(\frac{Ze}{\pi}\right)^2 \int d\mathbf{q}\frac{\omega}{\mathbf{q}^2} n(\omega)\,\mathrm{Im}\left(-\frac{1}{\epsilon(\mathbf{q},\omega)}\right), \tag{2}$$

where $n(\omega)=(e^{\beta\hbar\omega}-1)^{-1}$ is the Bose factor, u is the velocity, and Ze is the charge of the test particle. Here the frequency $\hbar\omega=E(\mathbf{p}')-E(\mathbf{p})$ is given by the energy transfer of the scattering of a particle from an initial state with energy $E(\mathbf{p})$ to a final state with energy $E(\mathbf{p}')$, and a momentum transfer of $\hbar\mathbf{q}=\mathbf{p}'-\mathbf{p}$. It should be stressed that Eq. (2) is valid for the case of weak coupling between the projectile and the plasma, given by the parameter $\eta=Ze^2/\hbar u_r \ll 1$ [16], where u_r is the electron-test particle relative velocity. Hence the dielectric formalism in linear response becomes exact in the limit of high test particle velocities. The aim of this work is to study the influence of an external magnetic field on the energy loss rate of an ion moving through a quantum plasma. In doing so we analyze the effect of the Larmor rotation of the test particle on the stopping power.

Our calculations are based on the description of the plasma in the random-phase approximation (RPA) and are therefore restricted to the weak-coupling limit of the interparticle correlations [17]. In order to describe a strongly coupled plasma system one must go beyond the RPA. This may be achieved by explicitly taking into account static and dynamic local-field corrections (LFC's) [18] in the dielectric function. Alternatively one may employ the method of frequency moments [19]. Other approaches also take into account a nonlinear coupling between the projectile and the plasma. They start from a quantum kinetic equation using a T-matrix approximation for the correlation effects between the test particle and the plasma [20,21]. All these approaches (except the investigations based on the method of moments [12,14]) are worked out only for nonmagnetized plasmas. It is difficult to generalize them to the case of a magnetized plasma. Therefore they go beyond the scope of this work.

However, it has been realized that the RPA serves as an appropriate starting point for the calculation of the stopping power.

The energy loss rate of a test particle in a magnetized plasma has been recently investigated in Refs. [3–5] (and references therein). In their investigations the motion of the test particle as well as the plasma were treated classically. Here, we use a quantum mechanical description (RPA) of the beam-particle interaction rather than a classical dielectric tensor. Unlike its classical counterpart the RPA dielectric function guarantees the convergence of the integral for short-range interactions and avoids some arbitrary cutoff procedure. Furthermore, we assume that the electrons give the main contribution to the stopping power.

In this paper we obtain numerical and analytical results for the energy loss of a fast moving particle in a magnetized plasma. In Sec. II we specify the parameters of the plasma under consideration and briefly outline the formulation of the stopping power in the dielectric formalism. In Sec. III we obtain expressions for the dielectric function of a magnetized plasma of all degeneracies. We also give simplified results for the limiting case of a nondegenerate plasma. Analytical results for the stopping power in the limit of high and low velocities are derived in Sec. IV. The Larmor rotation of the test particle is taken into account. Finally, in Sec. V, we present numerical results for the energy loss rate for various parameters of the plasma and compare these results to the asymptotic results derived in Sec. IV.

II. BASIC THEORETICAL TREATMENT

The plasma under consideration is subject to an external constant magnetic field, which is considered to be parallel to the z-direction $\mathbf{B}=(0,0,B)$. It may be specified by its temperature T and by the plasma frequency $\omega_p=\sqrt{4\pi ne^2/m}$, where n is the electron density. The influence of the ions on the projectile energy loss will be neglected throughout this paper. The motion of the electrons are characterized by the cyclotron frequency $\omega_c=eB/mc$ or the magnetic length $l_B=\sqrt{\hbar c/eB}$, where m is the electron mass.

We consider a test particle of mass M and charge Ze that moves with velocity components $\mathbf{u}=(u_z,\mathbf{u}_\perp)$ in a magnetized plasma. The incident angle of the motion of the particle with respect to the magnetic field is denoted by α, so that $u_z=u\cos\alpha$ and $u_\perp=u\sin\alpha$. We assume a mass of the particle $M\gg m$ such that a classical description of its motion is applicable. The particle moves on circular orbits perpendicular to the field with a frequency $\Omega_c=ZeB/Mc$, while the motion parallel to the field is not influenced by the field.

Let us now derive a general expression for the stopping power of a particle in a magnetized plasma. In doing so, we essentially follow the method that was developed in Ref. [22]. We first consider the case where the incident particle must be described quantum mechanically, and from that we extract an equation for the stopping power in which the motion of the test particle can be described classically, i.e., in the limit $\hbar\to 0$. In quantum mechanics the motion perpendicular to the magnetic field is quantized with the energy eigenvalues given by $E_\perp=\hbar\Omega_c(n+1/2)$ [23]. The full energy spectrum of the test particle can then be written as

$$E_{n,k_z,\sigma}=\hbar\Omega_c\left(n+\frac{1+\sigma}{2}\right)+\frac{\hbar^2k_z^2}{2M}. \tag{3}$$

The corresponding eigenstates are labeled by $N=(n,k_y,k_z,\sigma)$, where σ is the spin variable. In a first approximation, if the interaction of the test particle and the plasma is sufficiently weak, the inelastic scattering rate of a particle from the initial state $N=(n,k_y,k_z,\sigma)$ to the final state $N'=(n',k_y',k_z',\sigma')$ can be calculated from Fermi's golden rule. We find for the scattering rate

$$R(N\to N',\omega)=\int\frac{d\mathbf{q}}{(2\pi)^3}\left(\frac{4\pi Ze^2}{\mathbf{q}^2}\right)^2\frac{2\pi}{\hbar^2}S(\mathbf{q},\omega)\times|\langle N'|e^{i\mathbf{qr}}|N\rangle|^2|_{\hbar\omega=E_{n',k_z',\sigma'}-E_{n,k_z,\sigma}}, \tag{4}$$

where we have introduced the dynamical charge-charge structure factor $S(\mathbf{q},\omega)$ of the plasma. The Fourier transform of the wave functions are given by [24]

$$\langle N'|e^{i\,\mathbf{qr}}|N\rangle=F_{nn'}\left(\frac{q_\perp^2l_B^2}{2}\right)\delta_{k_y',k_y+q_y}\delta_{k_z',k_z+q_z}\delta_{\sigma,\sigma'}, \tag{5}$$

where

$$F_{nn'}(x)=\left[\frac{n!}{n'!}\right]^{1/2}x^{(n'-n)/2}\exp(-x/2)L_n^{n'-n}(x)\quad(n<n'),$$

$$F_{nn'}(x)=(-1)^{n-n'}F_{n'n}(x)\quad(n>n'), \tag{6}$$

and $L_n^{n'}(x)$ are the generalized Laguerre polynomial [25]. The classical motion of the test particle allows us to consider the matrix elements in the limit $\hbar\to 0$, with the result (see also [24])

$$F_{nn'}\left(\frac{q_\perp^2l_B^2}{2}\right)\to J_{n'-n}(q_\perp a), \tag{7}$$

with $a=u_\perp/\Omega_c$ and $J_n(x)$ being the Bessel function of order n. Using this relation and Eq. (4) it follows that

$$R(N\to N',\omega)=\int\frac{d\mathbf{q}}{(2\pi)^3}\left(\frac{4\pi Ze^2}{\mathbf{q}^2}\right)^2\frac{2\pi}{\hbar^2}S(\mathbf{q},\omega)\times J_{n'-n}^2(q_\perp a)\,\delta_{k_y',k_y+q_y}\delta_{k_z',k_z+q_z}\delta_{\sigma,\sigma'}\times\delta(E_{n,k_z,\sigma}-E_{n',k_z',\sigma'}+\hbar\omega). \tag{8}$$

The dynamical structure factor $S(\mathbf{q},\omega)$ can be obtained from the dielectric function $\epsilon(\mathbf{q},\omega)$ of the plasma, by using the fluctuation dissipation theorem [26] one finds

$$S(\mathbf{q},\omega)=\frac{\hbar\mathbf{q}^2}{4\pi^2e^2}n(\omega)\,\mathrm{Im}\left(-\frac{1}{\epsilon(\mathbf{q},\omega)}\right). \tag{9}$$

The energy transfer $\hbar\omega$ may be determined from

$$\hbar\omega=\hbar p_z u_z+\frac{\hbar^2 p_z^2}{2M}+s\hbar\Omega_c, \tag{10}$$

with $s=n'-n$ and $p_z=k_z'-k_z$. Since we assume a classical motion of the test particle, we can neglect the second term in this equation. The energy loss rate is given by a sum over all final states:

$$\frac{dE}{dt}=\sum_{N'}\hbar\omega R(N\to N',\omega). \tag{11}$$

In the next step we split the integral into $\omega>0$ and $\omega<0$ parts and make use of the relation $n(\omega)+n(-\omega)=-1$. With that we obtain for the stopping power in a magnetic field

$$\begin{aligned}S&=-\frac{1}{u}\frac{dE}{dt}\\&=\frac{2Z^2e^2}{\pi u}\sum_{s=-\infty}^{\infty}\int_0^\infty dq_\perp q_\perp J_s^2(q_\perp a)\int_{-\infty}^{\infty}dq_z\frac{q_z u_z+s\Omega_c}{q_\perp^2+q_z^2}\\&\quad\times\mathrm{Im}\left(-\frac{1}{\epsilon(q_z,q_\perp,q_z u_z+s\Omega_c)}\right)\Theta(q_z u_z+s\Omega_c),\end{aligned} \tag{12}$$

where $\Theta(\omega)$ is the well-known step function. Essentially, this equation describes the energy loss of a classical particle moving in a magnetic field and passing a magnetized quantum plasma. Alternatively, one can derive Eq. (12) from the linearized Vlasov equation, where the self-consistent electrostatic potential is determined by Poisson's equation. Since this is a classical derivation, the plasma dielectric function in Eq. (12) is given by its classical representation. This program was first carried out by Rostoker [27]. Additionally, one must introduce a momentum cutoff to avoid the divergence of the integral at small distances. In contrast to that, the description of the projectile plasma interaction used in this work leads to a quantum expression for the dielectric function and avoids the cutoff procedure at small distances, which is inherent in the classical treatment.

III. DIELECTRIC FUNCTION

In this section we obtain expressions for the dielectric function in random-phase approximation, including both thermal and quantum effects. We first introduce the polarization function $\Pi(\mathbf{q},\omega)$ which is connected to the dielectric function by the following expression:

$$\epsilon(\mathbf{q},\omega)=1+\frac{4\pi e^2}{\mathbf{q}^2}\Pi(\mathbf{q},\omega). \tag{13}$$

The polarization function describes the response of the plasma to a test charge. In general, the response of the system is calculated within a perturbation theory. The lowest order contribution is the RPA. In this approximation the polarization function is determined solely by a collisionless, i.e., noninteracting, Fermi system in a magnetic field, and it can be written in the form

$$\begin{aligned}\Pi(\mathbf{q},\omega)=\sum_\sigma\int\frac{dk_z}{(2\pi l_B)^2}&\\\times\sum_{n,n'}\sum_{k_y,k_y'}\frac{f(E_{n,k_z,\sigma})-f(E_{n',k_z+q_z,\sigma})}{\hbar\omega+E_{n,k_z,\sigma}-E_{n',k_z+q_z,\sigma}+i0^+}&\\\times|\langle n',k_y',k_z+q_z,\sigma|e^{i\,\mathbf{qr}}|n,k_y,k_z,\sigma\rangle|^2.&\end{aligned} \tag{14}$$

Here the summation is carried out over all Landau levels n,n' and spin variables σ. The arguments of the Fermi-Dirac function $f(E_{n,k_z,\sigma})$ are given by the eigenvalues of the free particles:

$$E_{n,k_z,\sigma}=\hbar\omega_c\left(n+\frac{1+\sigma}{2}\right)+\frac{\hbar^2k_z^2}{2m}. \tag{15}$$

The polarization function in a magnetic field in RPA, i.e., Eq. (14), has been extensively studied by Horing [28] within the Green's function method. He used a closed form of the polarization function, avoiding unwieldly summations over Landau eigenstates, and derived analytical results for different limiting cases. Since we are interested in the general case of arbitrary degeneracy, our starting point is the single particle wave function of a particle moving in a magnetic field. The results for the matrix elements have already been given in the previous section [Eq. (5)].

In the next step we separate $\Pi(\mathbf{q},\omega)$ into real and imaginary parts. This may be accomplished by using the identity

$$\frac{1}{\omega-\omega_0+i0^+}=P\frac{1}{\omega-\omega_0}-i\pi\delta(\omega-\omega_0). \tag{16}$$

We first find an expression for the imaginary part of the response function. The δ-function allows us to perform the k_z-integration in Eq. (14), and we readily obtain

$$\begin{aligned}\mathrm{Im}\,\Pi(\mathbf{q},\omega)=\frac{1}{4\pi l_B^2}\frac{m}{\hbar^2|q_z|}&\\\times\sum_\sigma\sum_{n,n'}[f(E_{n,m/\hbar q_z(\omega+\omega_c(n-n')-\hbar q_z^2/2m),\sigma})&\\-f(E_{n',m/\hbar q_z(\omega+\omega_c(n-n')+\hbar q_z^2/2m),\sigma})]&\\\times F_{nn'}^2\left(\frac{q_\perp^2 l_B^2}{2}\right).&\end{aligned} \tag{17}$$

This result is valid at arbitrary degeneracy of the plasma and may serve as a starting point for numerical analysis. In the next section we will find a simplified expression for the dielectric function in the limit of small degeneracy. Furthermore, we present an expression for the real part of the response function, which is obtained by using the Kramers-Kronig relation [26]. The result reads as

$$\mathrm{Re}\,\Pi(\mathbf{q},\omega)=\frac{1}{4\pi l_B^2}\frac{m}{\hbar^2|q_z|}\times\sum_{\sigma}\sum_{n,n'}\left[g(E_{n,m/\hbar q_z(\omega+\omega_c(n-n')-\hbar q_z^2/2m),\sigma})-g(E_{n',m/\hbar q_z(\omega+\omega_c(n-n')+\hbar q_z^2/2m),\sigma})\right]\times F_{nn'}^2\left(\frac{q_\perp^2 l_B^2}{2}\right),\tag{18}$$

where the function $g(E_{n,x(\omega),\sigma})$ is defined by

$$g(E_{n,x(\omega),\sigma})=P\int_{-\infty}^{\infty}d\omega'\frac{f(E_{n,x(\omega'),\sigma})}{\omega-\omega'}\tag{19}$$

and the integral is to be understood in the sense of a Cauchy principal value. It is useful to establish the relation between the chemical potential $\mu=\mu_N+N\hbar\omega_c$ and the particle density n, given by

$$n=\frac{2x}{\Lambda^3}\frac{1}{\sqrt{\pi}}{\sum_{N=0}^{\infty}}'\,F_{-1/2}(\beta\mu_N),\tag{20}$$

where the sum in Eq. (20) extends over all Landau levels N and the standard Fermi integrals $F_\nu(\alpha)$ are defined by

$$F_\nu(\alpha)=\int_0^\infty dx\frac{x^\nu}{e^{x-\alpha}+1}.\tag{21}$$

In the next section we give simplified results for the dielectric funciton of a nondegenerate plasma.

High-temperature, low-density plasmas. We can now obtain expressions for the real and imaginary part of the dielectric function of a high-temperature and low-density plasma. These plasmas are characterized by the relation $n\Lambda^3\tanh(x)/(2x)=e^{\mu/kT}\ll 1$, where $\Lambda=h/\sqrt{2\pi mkT}$, $x=\hbar\omega_c/2kT$, and μ is the chemical potential for the plasma electrons. In this case the Fermi-Dirac distribution can be replaced by the Boltzmann distribution. Notice that a magnetic field increases the domain of classical behavior ($e^{\mu/kT}\ll 1$) towards higher densities.

Our starting point for $\mathrm{Im}\,\Pi(\mathbf{q},\omega)$ is Eq. (17). The series $\Sigma_{n'}$ may be summed by using the representation of the modified Bessel function $I_N(x)$ in terms of the generalized Laguerre polynomials. After some lengthy calculations one arrives at the following expression for the imaginary part of the dielectric function [28]:

$$\mathrm{Im}\,\epsilon(\mathbf{q},\omega)=\frac{m\omega_p^2}{\hbar\mathbf{q}^2|q_z|}\left(\frac{2\pi m}{kT}\right)^{1/2}\sum_{n=-\infty}^{\infty}\times\exp\left[-\left(\frac{m(\omega-n\omega_c)^2}{2q_z^2}+\frac{\hbar^2q_z^2}{8m}\right)\Big/\,kT\right]\times\sinh\left(\frac{\hbar\omega}{2kT}\right)e^{-q_\perp^2l_B^2/2\coth x}I_n\left(\frac{q_\perp^2l_B^2}{2\sinh x}\right).\tag{22}$$

As expected, the zero field result [29] for $\mathrm{Im}\,\epsilon(\mathbf{q},\omega)$ is recovered along the magnetic field ($q_\perp=0$), where the sum in Eq. (22) is reduced to the term $n=0$.

Following the same steps described above we have also computed the real part of $\epsilon(\mathbf{q},\omega)$, with the result

$$\mathrm{Re}\,\epsilon(\mathbf{q},\omega)=1+\frac{m\omega_p^2}{\hbar\mathbf{q}^2|q_z|}\left(\frac{m}{2kT}\right)^{1/2}\sum_{n=-\infty}^{\infty}(e^{-nx}\Phi(s_+)-e^{nx}\Phi(s_-))\exp\left(-\frac{q_\perp^2l_B^2}{2}\coth x\right)I_n\left(\frac{q_\perp^2l_B^2}{2\sinh x}\right),\tag{23}$$

with $s_\pm=\sqrt{m\beta/2q_z^2}(\omega-n\omega_c\pm\hbar q_z^2/2m)$ and $\Phi(s)$ is the plasma dispersion function given by

$$\Phi(s)=\frac{1}{\sqrt{\pi}}P\int_{-\infty}^{\infty}dz\frac{e^{-z^2}}{s-z}=\sqrt{\pi}e^{-s^2}\,\mathrm{Erfi}(s).\tag{24}$$

Again, we observe the zero field results [29] for $\mathrm{Re}\,\epsilon(\mathbf{q},\omega)$ in the limit $q_\perp\to 0$.

Equations. (17), (18), (22), and (23) form the basis for the numerical analysis of the energy loss rate. These results are presented in Sec. V and are compared with the analytical results derived in the next section.

IV. ASYMPTOTIC RESULTS

We now focus our attention on the derivation of analytical results for the stopping power in limiting cases. We study the stopping power in dependence on the velocity of the charged paricle at both low velocities, $v\to 0$, and high velocities, $v\to\infty$. The influence of the Larmor rotation on the stopping power is discussed.

A. High-velocity limit

Let us consider the situation when the projectile velocity is much larger than the thermal velocity of the plasma electrons. In this high-velocity limit the damping effects can be neglected and consequently the imaginary part of the inverse dielectric function can be described by a sharp loss of energy at the plasma excitation frequencies $\pm\omega_{\mathbf{q}}$. These frequencies should be chosen in such a way that the corresponding dielectric tensor satisfies the frequency sum rules. In order to simplify the calculation we will divide the q-integration into a region of small momentum transfer, i.e., $q<q_{\max}$, and large momentum transfer $q>q_{\max}$ and will use different approximations for the energy loss function in each region. Clearly, the final result is independent of the particular choice of $q_{\max}$. For large distances, i.e., $q<q_{\max}$, we can use the cold plasma approximation for the inverse dielectric function, which is given by the expression

$$\mathrm{Im}\left(-\frac{1}{\epsilon(\mathbf{q},\omega)}\right)=\frac{\pi}{2}(\omega^2-\beta^2)\left(\frac{\omega_-}{\omega_-^2-\omega_+^2}\delta(\omega-\omega_-)-\frac{\omega_+}{\omega_-^2-\omega_+^2}\delta(\omega-\omega_+)\right), \tag{25}$$

with the plasma frequencies ω_- and ω_+ given by

$$\omega_\pm=(1+\beta^2)/2\pm\sqrt{(1+\beta^2)^2/4-\beta^2\cos^2\theta}, \tag{26}$$

where θ denotes the angle between the wave vector and the magnetic field. One can easily check that the inverse dielectric function defined in Eq. (25) satisfies the frequency sum rules. Notice, that all frequencies are measured in units of the plasma frequency ω_p. We have also introduced a measure of the electron cyclotron frequency, given by $\beta=\omega_c/\omega_p$. The approximation (25) describes a sharp loss of energy at the plasma excitation frequencies $\omega_\pm$. At small distances, i.e., $q>q_{\max}$, we can use

$$\mathrm{Im}\left(-\frac{1}{\epsilon(\mathbf{q},\omega)}\right)=\frac{\pi}{2}\frac{1}{\omega}[\delta(\omega-\omega_\mathbf{q})+\delta(\omega+\omega_\mathbf{q})], \tag{27}$$

where $\omega_\mathbf{q}$ is obtained from the fourth frequency moment and reads as $\omega_\mathbf{q}^2=(\hbar/2m\omega_p)^2\mathbf{q}^4$ [13]. These characteristic frequencies may be calculated from the dielectric function at high frequencies. Having introduced these general expressions we may now proceed to analyze the slowing down of a test particle passing a plasma for different incident angles α and physical situations.

1. Arbitrary direction and $\Omega_c=0$

In a first approach we neglect the curvature of the motion of the incident particle, but consider its motion in arbitrary direction. Let us briefly outline the steps leading to the final result. Since we are interested in the high-velocity limit, we can start with the high-velocity approximations (25) and (27) for the energy loss function. Considering first the large momentum part ($q>q_{\max}$), we insert the high velocity approximation in Eq. (2) and carry out all integrations. Additionally, we neglect all terms that vanish as $u\to\infty$ and obtain the following expression:

$$S=\frac{Z^2e^2\omega_p^2}{u^2}\ln\left(\frac{2mu}{\hbar q_{\max}}\right). \tag{28}$$

Performing the same procedure for the small momentum part, a straightforward calculation will lead to

$$S=\frac{Z^2e^2\omega_p^2}{u^2}\left(\ln\left(\frac{uq_{\max}}{\omega_p}\right)-f(\beta)\right), \tag{29}$$

where again terms that vanish as $u\to\infty$ are neglected. Combining both expressions the $\ln q_{\max}$ terms cancel and we find the following leading term for the stopping power at high velocities:

$$S=\frac{Z^2e^2\omega_p^2}{u^2}\left(\ln\left(\frac{2mu^2}{\hbar\omega_p}\right)-f(\beta)\right), \tag{30}$$

where the constant $f(\beta)$ is given by

$$f(\beta)=\frac{1}{2\pi}\int_0^{\omega_1}d\omega\frac{\omega|\beta^2-\omega|\ln\omega}{\sqrt{|\omega(\omega-\omega_1)(\omega-\omega_2)(\omega-\omega_3)|}}+\frac{1}{2\pi}\int_{\omega_2}^{\omega_3}d\omega\frac{\omega|\beta^2-\omega|\ln\omega}{\sqrt{|\omega(\omega-\omega_1)(\omega-\omega_2)(\omega-\omega_3)|}}, \tag{31}$$

with the characteristic frequencies determined by

$$\omega_{1\atop 2}=(1+\beta^2)/2\mp\sqrt{(1+\beta^2)^2/4-\beta^2\sin^2\alpha},\omega_3=1+\beta^2. \tag{32}$$

This result is the generalization of Bethe's expression for the stopping power in the high-velocity limit and was first derived by Akhiezer [1]. The constant $f(\beta)$ vanishes in the limit $\beta\to0$, from which one retrieves the zero field result. Akhiezer [1] also derived an analytical expression for $f(\beta)$ at arbitrary incident angles and at strong magnetic fields $\beta\gg1$, which reads

$$f(\beta)=\frac{1+\cos^2\alpha}{4}\ln(1+\beta^2)+\frac{\sin^2\alpha}{4}\left(1+\ln\frac{\sin^2\alpha}{4}\right). \tag{33}$$

Two general results can be extracted out of this expression concerning the influence of the magnetic field on the high-velocity stopping power for the zero curvature motion of the test particle. First, the stopping power of a plasma is reduced as a consequence of an increasing magnetic field strength. Furthermore, one must be careful by applying the high-velocity approximation in the infinite magnetic field case. The argument of the logarithmic term in Eq. (30) may be approximated by $2mu^2/\hbar(\omega_p^2+\omega_c^2)^{1/2}$, which must be a large quantity in order to make this derivation in logarithmic accuracy valid. Clearly, this contradicts the assumption of an infinite magnetic field. The second point is that the high-velocity stopping power is a monotonic function of the incident angle of the test particle, having its maximum at perpendicular motion, i.e., $\alpha=\pi/2$, and its minimum at parallel motion, i.e., $\alpha=0$. The limiting cases of parallel and perpendicular motion and the influence of the Larmor rotation of the test particle will be discussed in the next section.

2. Parallel motion ($\alpha=0$)

If the incident particle moves parallel to the magnetic field, the stopping power will be independent of the curvature of the motion of the test particle, i.e., of Ω_c. Under these conditions only the term $s=0$ in Eq. (12) contributes to the energy loss. Inserting Eqs. (25) and (27) into Eq. (12) and carrying out all integrations one arrives at an expression which is obtained from the calculation of the previous sec-

tion by setting $\alpha=0$ in Eqs. (30) and (31). The result, which is valid at arbitrary magnetic field, reads as

$$S=\frac{Z^2e^2\omega_p^2}{u_z^2}\ln\left(\frac{2mu_z^2}{\hbar\omega_p\sqrt{1+\beta^2}}\right). \tag{34}$$

Here the characteristic frequency ω_p of the zero field expression is replaced by $(\omega_p^2+\omega_c^2)^{1/2}$, which reduces the stopping power as a consequence of an increasing magnetic field strength. In contrast to the result in Ref. [4], our result does not tend to a constant value for high-intensity magnetic fields. Equation (34) is confirmed by numerical calculations as discussed in Sec. V. We underline that the high velocity limit requires first to take the limit $u\to\infty$ and then to take $\beta\to\infty$, and not vice versa. We stress that one obtains our result, Eq. (34), by taking the limit $u\to\infty$ and then $\beta\to\infty$ in Eq. (29) of Nersisyan's paper. This is a consequence of the use of the high-frequency approximation instead of the high-magnetic-field approximation for the dielectric function. Physically, one requires the argument in the logarithm to be essentially larger than unity.

The experiments for the stopping power in a magnetized plasma reported in Ref. [6] are the only experiments that we are aware of. We have made a comparison of the experimental data with our asymptotic formula. Unfortunately, the error bars in the experimental data are so large that the influence of the magnetic field is covered. We also could not find a comparison of the experimental data at zero magnetic field with the data at finite magnetic field in this paper. This would at least indicate the qualitative behavior. Our asymptotic formula, Eq. (34), predicts a reduction of the stopping power of the magnetized plasma investigated in Ref. [6] of about 30% in comparison with the nonmagnetized plasma. In order to compare the experimental data with theoretical data, the experiments should be carried out at higher magnetic fields or the accuracy of the experiments should be improved. Alternatively, the experimentalists may investigate the case of perpendicular motion, in which one should observe characteristic resonances in the stopping power (see the next section).

3. Perpendicular motion ($\alpha=\pi/2$)

In the case of perpendicular motion of the particle we distinguish the two different cases of finite and zero curvature. First we discuss the case in which the curvature of the fast moving particle is neglected. The integral expression (31) for $f(\beta)$ cannot be simplified in the general case. Therefore one must numerically integrate Eq. (31) in order to obtain the stopping power in the high velocity limit at arbitrary magnetic field strengths.

However, at strong magnetic fields ($\beta\ll 1$), one can perform the integration and finds from Eq. (33) by putting $\alpha=\pi/2$

$$S=\frac{Z^2e^2\omega_p^2}{u_\perp^2}\left(\ln\left(\frac{2mu_\perp^2}{\hbar\omega_p(1+\beta^2)^{1/4}}\right)-\frac{1}{4}\left(1+\ln\frac{1}{4}\right)\right). \tag{35}$$

Again, we mention that the energy loss of a particle moving perpendicular to the field is larger than for a particle moving parallel to the field.

The second case deals with the more general situation where the Larmor rotation of the fast moving particle is taken into account. Since we are interested in the asymptotic limit of high velocities it is sufficient to start with the δ-function approximation [Eqs. (25) and (27)] for the inverse dielectric function. We find for the stopping power

$$S=\frac{Z^2e^2\omega_p^2}{u_\perp^2}\frac{4}{\pi}\sum_{s=-\infty}^{\infty}\int d\omega\,\omega\int_0^{q_{\max}}dq \times\int_0^1 dz\,J_s^2(q\sqrt{1-z^2}/\gamma)\,\delta(s\gamma-\omega)\,\mathrm{Im}\,\epsilon^{-1}. \tag{36}$$

Here we have introduced the dimensionless parameter $\gamma=\Omega_c/\omega_p$, which measures the cyclotron frequency of the test particle in units of the plasma frequency ω_p. We perform the ω- and z-integration in order to find a numerical tractable expression for the stopping power. The result reads as

$$S=\frac{Z^2e^2\omega_p^2}{u_\perp^2}\frac{2}{\beta}\left(\sum_{s=0}^{[s_1]}+\sum_{s=[s_2]}^{[s_3]}\right)\int_0^{q_{\max}}dq\;J_s^2 \times(q\sqrt{|(s^2\gamma^2-1)(s^2\gamma^2-\beta^2)|}/(\beta\gamma))\frac{s^2\gamma^2|s^2\gamma^2-\beta^2|}{\sqrt{1+\beta^2-s^2\gamma^2}}, \tag{37}$$

with the characteristic frequencies given by

$$s_1=\begin{cases}1/\gamma^2, & \beta\geqslant 1\\ \beta^2/\gamma^2, & \beta<1\end{cases};\quad s_2=\begin{cases}\beta^2/\gamma^2, & \beta\geqslant 1\\ 1/\gamma^2, & \beta<1\end{cases};$$

$$s_3=(1+\beta^2)/\gamma^2.$$

The upper limits in the summation over s, given by $[s_1]$ and $[s_3]$, are determined by rounding s_1 and s_3, respectively, downwards to the nearest integer, while $[s_2]$ is obtained by rounding s_2 upwards to the nearest integer. As it was shown in the previous section, $q_{\max}$ turns out to be given by $q_{\max}=2mu_\perp^2/(\hbar\omega_p)$.

The stopping power as given in Eq. (37) shows a divergency at magnetic field strengths, for which the ratio $(1+\beta^2)^{1/2}/\gamma$ is an integer value. Physically, this divergency is due to a resonant coupling of two oscillators with the frequencies Ω_c, i.e., the incident test particle, and $(\omega_p+\omega_c)^{1/2}$, i.e., the plasma waves, respectively. Since we have neglected damping effects in our calcuation, these resonances have an infinite amplitude. Our result is in contrast to that of Ref. [4], in which Fig. 3 indicates that the resonances occur at $s^2\gamma^2=1$. Since these characteristic resonances should be experimentally observable, we suggest to compare the results with experiment.

In Fig. 1 we have plotted the stopping power given by Eq. (37) as a function of the inverse magnetic field $1/\gamma$ using a

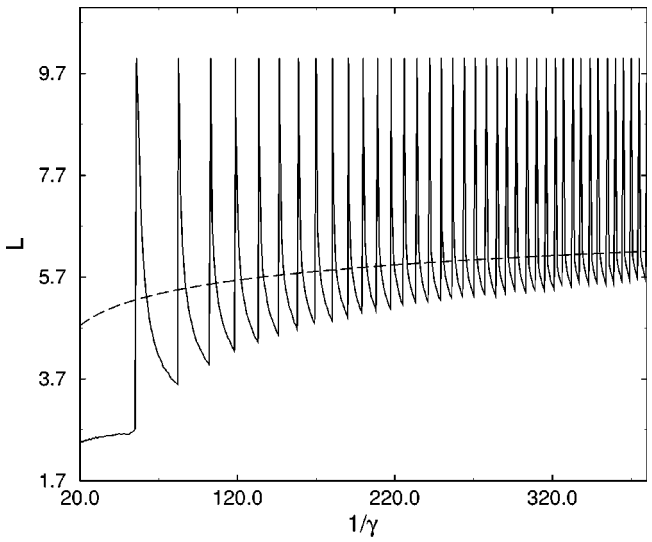

FIG. 1. Dependence of the stopping power [with $S=(Z^2e^2\omega_p^2/u_\perp^2)L$] on the inverse magnetic field strength $1/\gamma=\omega_p/\Omega_c$ in the high-velocity limit, assuming a finite curvature of the test particle and introducing some arbitrary cutoff. We have also included the asymptotic result for zero curvature, i.e., $\Omega_c=0$ (dashed line).

proton as a test particle, which is passing an electron plasma. In order to obtain a finite value for the stopping power we have cut the stopping power at some arbitrary value at the resonance frequencies. One also observes that the oscillations take place around the zero curvature result. In order to find the height and the width of the plasma resonances one must use a theory which goes beyond the sharp resonance approximation used in this work and which must include damping effects. One expects that the resonance peaks are observable at strong magnetic fields only and are damped out at small magnetic fields approaching the zero curvature asymptotics.

Notice that one can obtain the zero curvature results [Eqs. (30) and (31)] from Eq. (37) by performing the following steps. First, at small values of γ we can transform the summation into an integration according to $\Sigma_s f(s\gamma)=\int ds\, f(s\gamma)$. In a second step we use the relation $\int_0^{q_{\max}} J_{s/\gamma}^2(q/\gamma)\approx \ln q/s$, which is valid for $q_{\max}\to\infty$ and $\gamma\to 0$. Using these relations one readily arrives at Eq. (30).

B. Low-velocity limit

In the low-velocity limit one assumes that the projectile velocity is much smaller than the thermal velocity of the plasma electrons.

We remind the reader that the dielectric formalism employed in this paper is only valid if the velocity u of the projectile satisfies the inequality $u\gg Ze^2/\hbar$. In order to observe the low-velocity limit, the inequality $u\ll\sqrt{kT/m}$ should be satisfied. As a consequence of these inequalities the temperature should be larger than $T\gg Z\times 10^5$ K. Nevertheless, even for a low-temperature plasma the stopping power obtained in the dielectric formalism is the basic quantity for the calculation of the total stopping power (see [19], and references therein). Additionally, the low-velocity limit of the stopping power is closely connected to transport properties such as the conductivity. It may also be used to calculate transport properties avoiding the solution of complicated kinetic equations. In the dielectric formalism we can apply the low-frequency approximation for the dielectric function [22] to obtain the low-velocity limit. We have for the real part

$$\mathrm{Re}\,\epsilon(\mathbf{q},0)=1+\frac{q_s^2}{\mathbf{q}^2}, \tag{38}$$

where q_s is the inverse screening length. It is given by the first derivative of the particle density (20) with respect to the chemical potential, i.e., $q_s^2=4\pi e^2(\partial n/\partial\mu)$. Within this approximation $\mathrm{Re}\,\epsilon(\mathbf{q},0)$ shows an isotropic behavior. Anisotropy effects will be apparent by considering higher order terms. In general, it is appropriate to distinguish between a degenerate and a nondegenerate plasma. For a nondegenerate plasma one finds that the screening length is given by the inverse Debye radius k_D with

$$q_s^2=k_D^2=4\pi ne^2/kT. \tag{39}$$

For a degenerate plasma ($T=0$) one can approximate the screening length by the static Thomas-Fermi wave vector, which reads

$$q_s^2=\frac{1}{l_B a_B}\frac{\sqrt{2}}{\pi}\sum_{N=0}^{N_F}\frac{1}{\sqrt{1/t-N}}, \tag{40}$$

where t is the ratio of the Landau energy and the Fermi energy, given by $t=\hbar\omega_c/\epsilon_F$. N_F is the number of occupied Landau levels, i.e., it is the largest number for which the relation $N_F\hbar\omega_c<\epsilon_F$ is valid. Expressions for the Thomas-Fermi wave vector at finite temperatures can be found in [30].

We use an alternative expression for the low frequency approximation of the imaginary part [see [28], p. 38, Eq. (IV.1)] of the dielectric function, given by

$$\begin{aligned}\mathrm{Im}\,\epsilon(\mathbf{q},\omega\to 0)&=\frac{4\pi e^2}{\mathbf{q}^2}\left(\frac{m}{2\pi}\right)^{3/2}\frac{\hbar\omega_c}{2}\omega\int_{-\infty}^{\infty}dr\int_0^{\infty}d\omega'\frac{f_0(\omega')}{\hbar^3}\int_{\delta-i\infty}^{\delta+i\infty}\frac{ds}{2\pi i}\\&\times e^{\omega' s}\frac{\sqrt{s}}{\tanh\hbar(\omega_c/2)s}\exp\left(-\frac{q_z^2}{8ms}(\hbar^2s^2+r^2)\right)\\&\times\exp\left(-\frac{\hbar q_\perp^2}{2m\omega_c}\frac{\cosh\hbar(\omega_c/2)s-\cos(\omega_c/2)r}{\sinh\hbar(\omega_c/2)s}\right).\end{aligned} \tag{41}$$

This closed form for $\mathrm{Im}\,\epsilon(\mathbf{q},\omega\to 0)$ is appropriate to calculate the stopping power in the limiting case of weak and strong magnetic fields. At low velocities, we can further approximate the energy loss function by $\mathrm{Im}(-1/\epsilon(\mathbf{q},0))=-\mathrm{Im}\,\epsilon(\mathbf{q},\omega)/(\mathrm{Re}\,\epsilon(\mathbf{q},0))^2$. With this, we can find analytical

results for the nondegenerate and degenerate plasma. In both cases we obtain the characteristic dependence of the stopping power on the projectile velocity. This linear dependence of the energy loss of a slow particle is a consequence of the heavy particle limit $M\to\infty$, considered in this paper. It is a general result and is not restricted to the RPA. The RPA manifests itself only in the proportionality factor, which depends on the chosen approximation.

1. Nondegenerate plasma

At low velocities we find the following expression for the stopping power

$$S=\frac{2}{3}\frac{(2\pi m)^{1/2}}{(kT)^{3/2}}Z^2e^4nCu, \tag{42}$$

where the proportionality factor in its general form is given by

$$C=\left(\frac{9}{2\pi^3}\right)^{1/2}\int_0^\infty dq\int_{-1}^1 dz\int_{-\infty}^\infty dr\frac{q^4}{(q^2+y^2)^2}\times\exp\left[-q^2\left(\frac{z^2}{8}+\frac{1-z^2}{4x\sinh(x)}(\cosh(x)-\cos(xr))+\frac{z^2r^2}{8}\right)\right]\frac{\pi}{4}(2z^2\cos^2(\alpha)+(1-z^2)\sin^2(\alpha)). \tag{43}$$

Here we have introduced the two dimensionless parameters $y=\hbar\omega_p/kT$ and $x=\hbar\omega_c/2kT$. Additionally, the stopping power will also depend on the direction of the propagation of the particle. In the limit $x\to 0$, Eq. (43) reduces to the known result [22]. The first correction term to the zero field result may also be calculated analytically. This contribution will be in quadratic order with respect to the magnetic field, due to the symmetry of the system. The strong field limit is extracted from Eq. (43) by performing a saddle point approximation of the r-integration. All results are summarized in the following equation:

$$C=\begin{cases}(1+y^2/8)e^{y^2/8}E_1(y^2/8)-1, & x=0\\ [(1+y^2/8)e^{y^2/8}E_1(y^2/8)-1]+\dfrac{x^2}{240y^2}(1+\sin^2(\alpha))\{48+y^4-(y^6/8+y^4-2y^2)e^{y^2/8}E_1(y^2/8)\}, & x<1\\ \dfrac{3}{2}\cos^2(\alpha)e^{y^2/8}E_1(y^2/8) \quad \text{if} \quad \alpha\approx 0; \quad \dfrac{3}{8}\sin^2(\alpha)x^2 \quad \text{if} \quad \alpha>0, \quad x>1.\end{cases}$$

For a nondegenerate plasma one usually deals with the situation $y\ll 1$. Using these results we establish now some equations for the limit $y\to 0$, which read

$$C=\begin{cases}-\ln(y^2/8)-\mathbf{C}-1, & x=0\\ -\ln(y^2/8)-\mathbf{C}-1+\dfrac{x^2}{5y^2}(1+\sin^2(\alpha)), & x<1\\ -\dfrac{3}{2}\cos^2(\alpha)(\mathbf{C}+\ln(y^2/8)) \quad \text{if} \quad \alpha\approx 0; \quad \dfrac{3}{8}\sin^2(\alpha)x^2 \quad \text{if} \quad \alpha>0, \quad x>1,\end{cases}$$

where $\mathbf{C}\approx 0.5772$ is Euler's constant. At low velocities the stopping power of the plasma increases as a result of an increasing magnetic field strength, in contrast to the high-velocity limit, where the energy loss decreases.

2. Degenerate plasma

The case of a slow test particle passing a degenerate plasma was first considered by Fermi and Teller [31]. They derived a linear dependence of the stopping power on the test particle velocity. This linear dependence also holds in the case of a magnetized plasma

$$S=\frac{2}{3\pi}\frac{m^2Z^2e^4}{\hbar^3}C_du. \tag{44}$$

This regime is characterized by the ratio of the Landau energy and the Fermi energy, given by $t=\hbar\omega_c/\epsilon_F$. Again, for vanishing field we retrieve the known result [22]. Similarly as described in the previous section one may obtain analytical results in the limit of weak and strong magnetic fields. The results read as

$$C_d=\begin{cases}\ln(1+1/X_0)-\dfrac{1}{1+X_0}, & t=0\\ \ln(1+1/X_0)-\dfrac{1}{1+X_0}+t^2\left[\dfrac{1}{24}\dfrac{3X_0-1}{(1+X_0)^3}+\dfrac{1}{120}(1+\sin^2(\alpha))\dfrac{21X_0^2-2X_0+1}{(1+X_0)^4}\right], & t<1\\ t\dfrac{3}{4}\dfrac{\cos^2(\alpha)}{1+X_B} \quad \text{if} \quad \alpha\approx 0; \quad \dfrac{3}{64}t^3\sin^2\alpha \quad \text{if} \quad \alpha>0, \quad t>1, \end{cases}$$

where $X_0=q_s^2/(4q_F^2(B=0))$ and $X_B=q_s^2/(4q_F^2)$. The Fermi wave vector q_F is in implicit form given in Eq. (20). In the strong field limit, $t>1$, one finds the simple relation $q_F=2\pi^2 l_B^2 n$ for the Fermi wave vector and $q_s^2=m\omega_p^2/2\epsilon_F$ for the Thomas-Fermi wave vector. Again, we find an increase of the energy loss as a consequence of an increasing magnetic field.

V. NUMERICAL RESULTS AND DISCUSSION

We now proceed with presenting numerical results for the stopping power neglecting the curvature of the test particle. The numerical results were obtained from Eq. (2), using the full dielectric function as discussed in Sec. II. The energy loss of a particle moving parallel to the magnetic field as a function of its velocity for various field strengths is shown in Fig. 2. We have also included the zero field result and the asymptotic result at high velocities [Eq. (30)] derived in Sec. IV. The stopping power decreases with increasing magnetic field strength at high velocities. The low-velocity limit is essentially given by the zero field result, since $\hbar\omega_c/2kT\ll 1$. One also observes a peak in the stopping power at around the thermal velocity of the electrons, which becomes narrower at stronger magnetic fields. This is due to the fact that at low velocities the stopping power is essentially given by the zero field result, while at high velocities it approaches a different asympotic result.

The stopping power as a function of the inverse magnetic field for various incident angles is plotted in Fig. 3. At high velocities the stopping power is a monotonic function of the incident angle, reaching the maximum value at perpendicular motion and the minimum value at parallel motion of the test particle with respect to the magnetic field. The high-velocity limits are found to be well-reproduced by Eqs. (30) and (31).

VI. CONCLUSION

In this paper we have concentrated on the quantum mechanical treatment of the energy loss of a test particle in a plasma under the influence of a constant uniform magnetic field. We have considered the influence of the magnetic field on the plasma (plasma frequency, etc.) as well as on the motion of the heavy particle. All results were obtained within the dielectric formalism, using a RPA dielectric function. We have derived analytical results in the limit of high- and low-particle velocities. It was found that at high velocities the magnetic field reduces the stopping power, while at

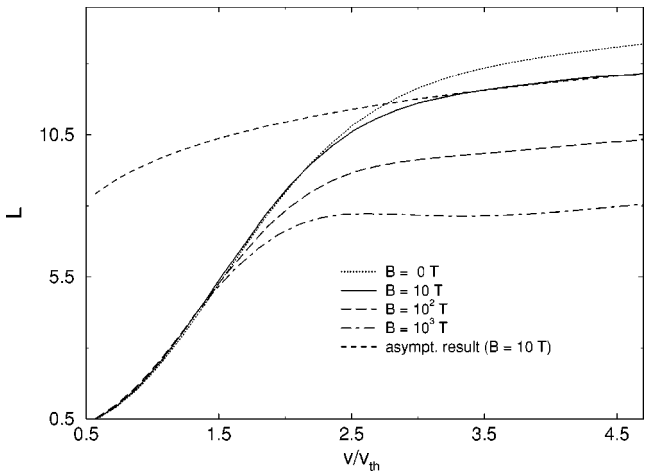

FIG. 2. Numerical results for the stopping power parallel to the magnetic field [with $S=(Z^2e^2\omega_p^2/u_z^2)L$] versus velocity [$u_{th}=(kT/m)^{1/2}$ is the thermal velocity of the plasma electrons] for various magnetic field strengths at a density of $n=10^{20}$ m^{-3} and a temperature of $T=10^5$ K. We have also included the zero field results and the asymptotic behavior (33) for $B=10$ T.

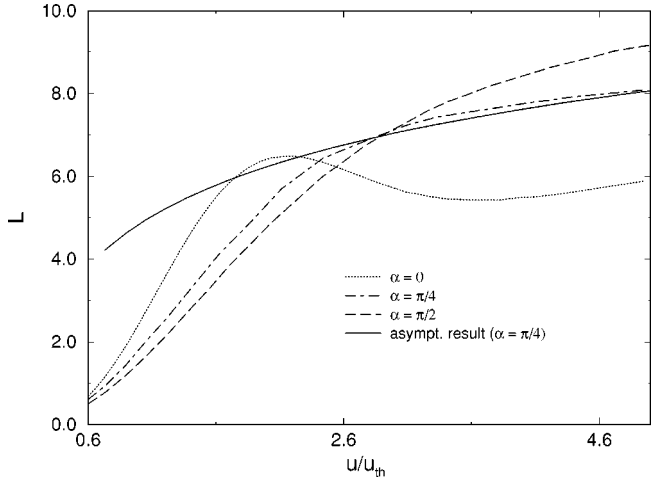

FIG. 3. The stopping power [with $S=(Z^2e^2\omega_p^2/u^2)L$] as a function of the velocity (u_{th} is the thermal velocity of the plasma electrons) for various angles between the magnetic field and the direction of the incident particle. The electron density and temperature are $n=10^{20}$ m^{-3} and $T=10^5$ K, respectively. The magnetic field strengths is $B=10^4$ T. The solid line represents the asymptotic behavior [Eqs. (30) and (31)] for $\alpha=\pi/4$.

low velocities the magnetic field increases the energy loss rate. Additionally, we have shown that at high velocities the energy loss of the test particle perpendicular to the field is larger than parallel to the field. In order to remove the velocity constraints, we have also performed a numerical integration and have found that the asymptotic result at high velocities is well-reproduced by the analytical formula [Eqs. (30) and (31)]. The very good agreement of the numerical data with our asymptotic formula at high velocities is another strong argument that first taking the limit $u \to \infty$ and then $\beta \to \infty$ is the right order to obtain the high-velocity stopping power of a magnetized plasma.

Furthermore, we have analyzed the influence of the Larmor rotation of the test particle on the energy loss. We have demonstrated that at high velocities the energy loss shows a resonant behavior at $s^2\gamma^2 = 1 + \beta^2$, where s is an integer value. This behavior has its origin in the coupling of two oscillators with frequencies Ω_c and $(\omega_p^2 + \omega_c^2)^{1/2}$.

Finally, we have found analytical results for the stopping power in the low-velocity limit at both weak and strong magnetic field, although neglecting the curvature of the test particle.

ACKNOWLEDGMENTS

The authors thank I. M. Tkachenko and W. Ebeling for stimulating discussions. This work was supported by the Deutsche Forschungsgemeinschaft.

[1] I.A. Akhiezer, Zh. Eksp. Teor. Fiz. **40**, 954 (1961).
[2] N. Honda, O. Aoni, and T. Kihara, J. Phys. Soc. Jpn. **18**, 256 (1963).
[3] O. Boine-Frankenheim and J. D'Avanzo, Phys. Plasmas **3**, 792 (1996).
[4] H.B. Nersisyan, Phys. Rev. E **58**, 3686 (1998).
[5] C. Cereceda, C. Deutsch, M. De Peretti, M. Sabatier, and H.B. Nersisyan, Phys. Plasmas **7**, 2884 (2000).
[6] T. Winkler, K. Beckert, F. Bosch, H. Eickhoff, B. Franzke, F. Nolden, H. Reich, B. Schlitt, and M. Steck, Nucl. Instrum. Methods Phys. Res. A **391**, 12 (1997).
[7] F. Cornu, Europhys. Lett. **37**, 591 (1997); Phys. Rev. E **58**, 5268 (1998); **58**, 5293 (1998); **58**, 5322 (1998).
[8] D. Boose and A. Perez, Phys. Lett. A **234**, 113 (1997).
[9] M. Steinberg, J. Ortner, and W. Ebeling, Phys. Rev. E **58**, 3806 (1998); M. Steinberg, W. Ebeling, and J. Ortner, *ibid.* **61**, 2290 (2000).
[10] P. Skudlarski and G. Vignale, Phys. Rev. B **48**, 8547 (1993).
[11] M. Steinberg and J. Ortner, Phys. Rev. B **58**, 15460 (1998); *ibid.* **59**, 12693 (1999).
[12] J. Ortner, V.M. Rylyuk, and I.M. Tkachenko, Phys. Rev. E **50**, 4937 (1994).
[13] V.M. Rylyuk, J. Ortner, and I.M. Tkachenko, An. Fis. **94**, 23 (1998).
[14] I.M. Tkachenko, J. Ortner, and V.M. Rylyuk, Phys. Rev. E **57**, 4846 (1998).
[15] J. Lindhard, K. Dan. Vidensk. Selsk. Mat. Fys. Medd. **28**, 3 (1954).
[16] G. Zwicknagel, Ch. Toepffer, and P.-G. Reinhardt, Phys. Rep. **309**, 177 (1999).
[17] G. Maynard and C. Deutsch, Phys. Rev. A **26**, 665 (1982).
[18] X.-Z. Yan, S. Takanaka, S. Mitake, and S. Ichimaru, Phys. Rev. A **32**, 1785 (1985).
[19] J. Ortner and I. M. Tkachenko, Phys. Rev. E (to be published).
[20] D.O. Gericke and M. Schlanges, Phys. Rev. E **60**, 904 (1999).
[21] K. Morawetz and G. Röpke, Phys. Rev. E **54**, 4134 (1996).
[22] N. Arista and W. Brandt, Phys. Rev. A **23**, 1898 (1981).
[23] L.D. Landau and E.M. Lifshitz, *Quantum Mechanics* (Pergamon, Oxford, 1958).
[24] N.D. Mermin and E. Canel, Ann. Phys. (N.Y.) **30**, 249 (1964).
[25] I.S. Gradstein and I.M. Ryshik, *Summen-, Produkt- und Integraltafeln* (Verlag der Wissenschaften, Berlin, 1957).
[26] L.D. Landau and E.M. Lifshitz, *Statistical Physics, Part II* (Pergamon, Oxford, 1986).
[27] N. Rostoker, Phys. Fluids **3**, 922 (1960).
[28] N.J. Horing, Ann. Phys. (N.Y.) **31**, 1 (1965).
[29] N. Arista and W. Brandt, Phys. Rev. A **29**, 1471 (1984).
[30] N.J. Horing, Ann. Phys. (N.Y.) **54**, 405 (1969).
[31] E. Fermi and E. Teller, Phys. Rev. **72**, 399 (1947).